

Nanoengineered device for drug delivery application

Piyush M Sinha¹, George Valco¹, Sadhana Sharma², Xuewu Liu²
and Mauro Ferrari^{2,3}

¹ Department of Electrical and Computer Engineering, The Ohio State University,
2015 Neil Avenue, Columbus, OH 43210, USA

² Dorothy M Davis Heart and Lung Research Institute, The Ohio State University,
473 West 12th Avenue, Columbus, OH 43210, USA

³ Department of Internal Medicine, Division of Hematology and Oncology,
The Ohio State University, Columbus, OH 43210, USA

E-mail: sinha.34@osu.edu

Received 9 March 2004

Published 23 July 2004

Online at stacks.iop.org/Nano/15/S585

doi:10.1088/0957-4484/15/10/015

Abstract

A high precision nanoengineered device was developed to yield long term zero-order release of drugs for therapeutic applications. The device contains nanochannels that were fabricated in between two directly bonded silicon wafers and therefore poses high mechanical strength. The fabrication is based upon selectively growing oxide and then removing it, and thus defining nanochannels by consuming a specified layer of silicon during oxide growth. Diffusion through the nanochannels is the rate limiting step for the release of drugs. A measurement of glucose released through such nanochannels validates the zero-order release profile. Device design, fabrication details and the glucose release profile through 60 nm channels are presented.

1. Introduction

Considerable advances have been made in the field of drug delivery technology over the last three decades, resulting in many breakthroughs in clinical medicine [1–3]. However, important classes of drugs have yet to benefit from these technological successes. One of the major requirements for implantable drug delivery devices is controlled release of therapeutic agents, especially biological molecules, as a continuous delivery over an extended period of time. The goal here is to achieve a continuous drug release profile consistent with zero-order kinetics where the concentration of the drug in blood remains constant throughout the delivery period. Injected drugs have first-order kinetics, with initial high concentration in blood (above the therapeutic range), followed by an exponential fall. Toxicity occurs when the peak concentration is above the therapeutic range, while efficacy of the drug diminishes as the drug concentration falls below this range. Therefore, the therapeutic advantages of continuous release of the drug by implantable delivery devices are significant—minimized adverse reactions by reducing the peak

levels, predictable and extended duration of action, reduced inconvenience of frequent dosing, and thereby improved patient compliance.

Different technologies have been developed to achieve this goal. However, they suffer from major drawbacks. Degradable polymer implants exhibit an initial ‘burst effect’ prior to sustained release and are typically not as efficient in controlling release rates of small molecules [4]. Implantable devices with percutaneous components such as ambulatory peritoneal dialysis, catheters, intravenous catheters, and orthopaedic implants are often associated with different failure modes. Infection, marsupialization, permigration, and avulsion are common occurrences [5]. Osmotic pumps lack the capabilities of electronic integration for achieving higher levels of functionality (i.e. pre-programming and remote activation) and are limited with respect to the type of drug they can deliver.

Silicon microfabrication technology can permit the creation of drug delivery devices that possess a combination of structural, mechanical, and electronic features that may surmount some of these challenges [1, 6]. Ease of

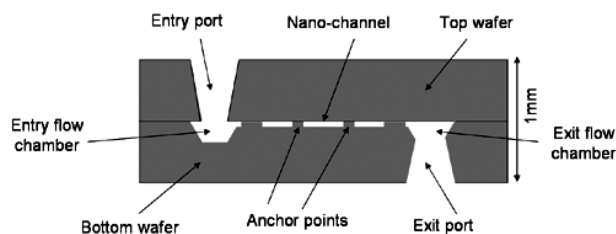


Figure 1. A cross-sectional view of the sandwich structure nanoporous membrane.

reproducibility, tightly controlled dimensions, and ability to manufacture in high volume are other advantages.

A nanochannel filter fabricated between two silicon substrates is a potential solution for this application, proposed in [7, 8]. This device offers good control of channel size and pore distribution, making it possible to control the release rate. The level of integration that can be achieved on a single silicon substrate provides major advantages over other materials used for making drug delivery devices. These sandwich structure nanochannel filters are fabricated using photolithography, selective oxide growth, and removal.

We have envisioned nanochannel delivery systems, or nDSs, for the delivery of therapeutic molecules. These devices will present progressively increasing degrees of functionality. The fundamental embodiment of the first device, nDS1, employs high precision nanoengineered channels to yield the long term zero-order release. nDS1 offers simplified device design and reduced fabrication steps compared to the devices proposed in [7, 8] that will allow high volume production at lower cost. Further, the device dimensions were optimized for high mechanical strength so that they are suitable for implantation. The mechanical strength analysis of this device is reported in a concurrent publication [9].

In this study we present the device design, fabrication details, and the test results of glucose release through the nanochannels of this device (nDS1). Some of the suggested applications of this device are the controlled release of cytokine interferon alpha-2b for the treatment of metastatic melanoma, and release of tacrolimus for immunosuppression during and after lung transplantation. We hypothesize that delivery of these agents from an nDS1 will improve the therapeutic efficacy of the medications, increase patient compliance, and minimize associated toxic effects compared to current methods of drug administration.

2. Device design

The sandwich structure nanochannel devices were fabricated using two silicon substrates. The silicon substrates were micromachined and then bonded together. The nanochannels exist between the two bonded silicon wafer surfaces. A cross-sectional view of the device is drawn in figure 1. The top substrate has an entry port that is etched all the way through the wafer, and aligns with the entry flow chamber on the bottom substrate. The bottom substrate contains the rest of the features. A top view of the bottom substrate is drawn in figure 2. This includes anchor regions along the edges and anchor points at many places between the nanochannels, where the top substrate is bonded to the bottom substrate.

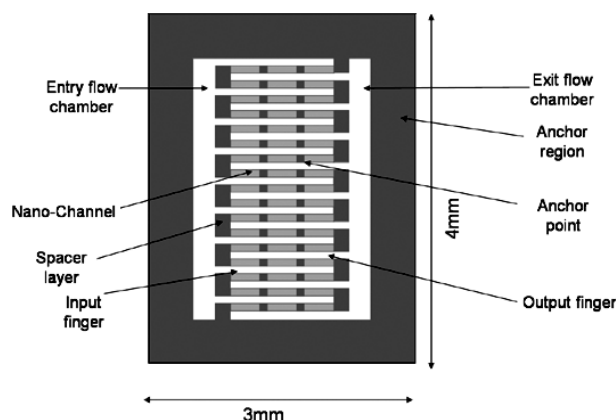


Figure 2. A top view of the sandwich structure nanoporous membrane.

Interdigitated input and output fingers open into the edges of the entry and exit flow chambers, respectively, with the nanochannels connecting between them. The drug being delivered comes to the entry flow chamber in the bottom substrate through the entry port in the top substrate, passes to the input fingers, and diffuses through the nano-channels to the output fingers and then to the exit flow chamber. The exit port that is aligned to the exit flow chamber in the bottom substrate provides a means for the drug to leave the device. The spacer layer at the tip of the fingers closes the fingers so that all drugs must flow through the nanochannels. The interdigitated design of several fingers with many nanochannels connecting them increases the drug flux. The nanochannel height defines the delivery rate limit. The effective porosity of the device depends upon the number, length, and width of the nanochannels, the width and periodicity of the anchor points, and the channel height. These geometries can be changed to design a desired flow rate.

The concept of nanochannel fabrication is based upon selectively growing oxide while consuming silicon during growth, and then etching the oxide layer (called sacrificial oxide). The nanochannel depth is defined as $d = 0.46t_{ox}$. Dry oxidation with a well controlled temperature and time allows precise control of the nanochannel's height.

The overall device dimensions were chosen to be 4 mm × 3 mm × 1 mm. In practice this device is mounted on a carrier that is placed in a cylindrical titanium capsule for the purpose of implantation in the body. The carrier divides the volume inside the capsule into two chambers, with the only connection between the chambers being by diffusion through the nanochannel device. The drug is contained in the chamber below the carrier and nanochannel device. The chamber above the nanochannel device is open to the body via a central opening through the wall of the titanium cylinder, of size comparable to the nanochannel device. The small size of the capsule allows for relatively simple subcutaneous insertion in the arm or abdomen. Titanium alloy as an implantable capsule is currently being used in DUROS[®] implant (Alza Corporation) that is an osmotic pump based drug delivery device.

The internal dimensions of the nanochannel device were optimized for high mechanical strength, so that it would not break in a body, if implanted. The mechanical strength analysis

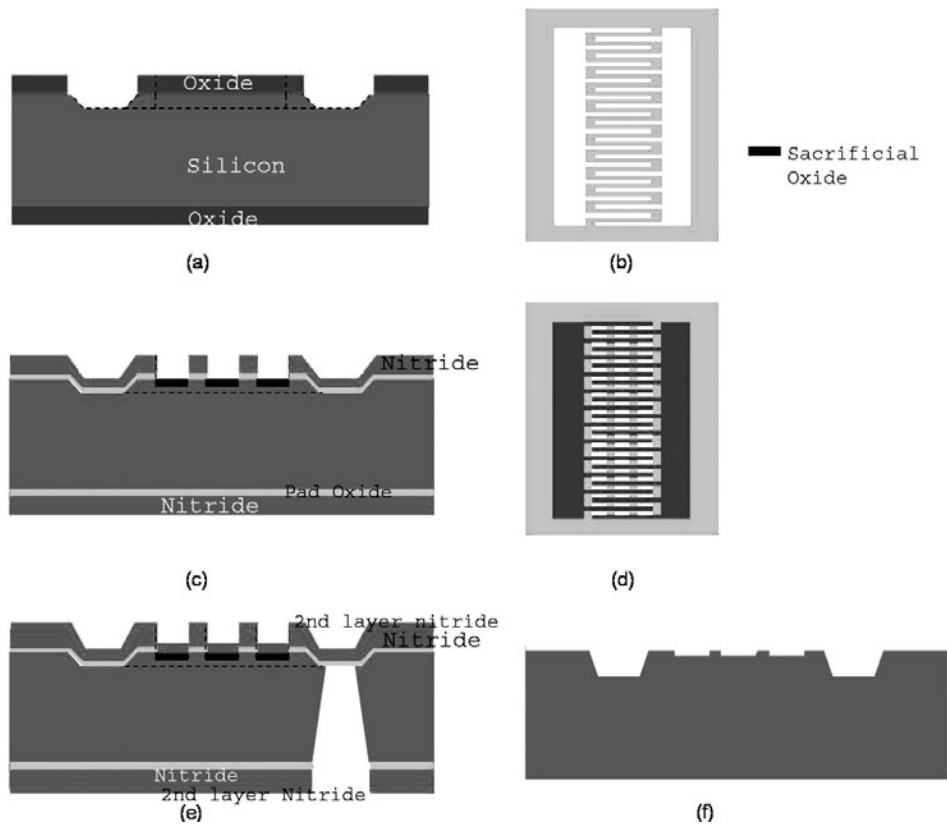


Figure 3. (a) Flow chambers and fingers, (b) mask 1 defining flow chambers and fingers, (c) nanochannels and anchor points, (d) mask 2 defining nanochannels and anchor points, (e) nanochannels protected by second layer of nitride and exit port (deep etch), and (f) complete bottom substrate fabrication.

was done considering the impact a person may experience in a car accident. The mechanical strength study is being reported in a concurrent publication. Here we present the fabrication details of the device and the glucose release profile through the nanopores.

3. Device fabrication

Double-side polished (100) single-crystal 4" silicon wafers were used for fabrication. The overall fabrication process can be divided into three major steps: (1) bottom substrate processing, (2) top substrate processing, and (3) wafer bonding and packaging.

3.1. Bottom substrate processing

Figure 3 shows the process flow for the bottom substrate fabrication. The first step was the fabrication of the entry flow chamber, exit flow chamber, input fingers, and output fingers. Oxide was used as a mask layer. This 0.5 μm thick oxide was grown in a H_2O ambient. The above-mentioned features were photolithographically defined using mask 1. The mask oxide was etched in the defined areas using a $\text{He} + \text{CHF}_3 + \text{CF}_4$ plasma. The features were then etched into silicon using 45 wt% $\text{KOH}:\text{H}_2\text{O}$ solution heated at 70°C . The mask oxide was then stripped in concentrated HF solution before proceeding to the next step.

Nanochannels were defined and fabricated in the next step. The sacrificial oxide for the nanochannels can

be grown thermally in a dry oxygen ambient with $\pm 1\%$ uniformity. The most common mask against such a local oxidation process is silicon nitride, which was used here. A pad oxide of 220 \AA thickness was first grown thermally by dry oxidation. The pad oxide reduces the stress between the silicon and silicon nitride layers and therefore enhances the adhesion of the two layers. A low stress LPCVD (low pressure chemical vapour deposition) nitride was then deposited using dichlorosilane (DCS) and NH_3 (100DCS/25 NH_3 /140 mTorr/ 835°C) on top of the pad oxide. The deposited nitride thickness was ~ 2200 \AA . The nanochannel regions were defined photolithographically using mask 2. The region between two nanochannels is an anchor point where the top substrate bonds to the bottom substrate. The nitride layer was etched in the defined areas using $\text{He} + \text{SF}_6$ plasma. This etch was controlled so that the underlying pad oxide does not get etched so that the silicon surface is not etched. This is very important in order to achieve good control of the nanochannel height. Then the pad oxide in the open areas was selectively (against silicon) etched in 25:1 HF . Once the silicon surface was exposed, a thermal oxide was grown to the desired thickness. This oxide growth defines the nanochannel size as mentioned earlier. Sacrificial oxide of thickness 130 nm was grown to give a 60 nm channel.

The final photolithography step for bottom wafer processing was for the exit port that was deep etched from the bottom side of this wafer. The exit port aligns to the exit flow chamber. Another layer of LPCVD nitride was deposited (same deposition conditions). The deposited nitride



Figure 4. Entry port in top substrate processing.

thickness was ~ 120 nm. This nitride protects the oxide in the nanochannel regions from being etched in the subsequent process. Backside photolithography was then performed to define the region of the exit port. The mask nitride and underlying pad oxide were etched in the defined area using $\text{He} + \text{SF}_6$ plasma. This etch was performed until the silicon surface was exposed. A deep etch was then performed in 45 wt% $\text{KOH}:\text{H}_2\text{O}$ solution heated at 80°C . The mask layer nitride, underlying pad oxide, and sacrificial oxide in the nanochannel region were stripped afterwards in concentrated HF solution.

3.2. Top substrate fabrication

The entry port was fabricated in the top substrate using a deep etch completely through the silicon wafer as shown in figure 4. Nitride was used as the mask for this deep etch. A pad oxide of 22 nm thickness was first grown in by dry thermal oxidation, and then LPCVD nitride (same deposition conditions as described earlier) of thickness ~ 340 nm was deposited. The entry port region was photolithographically defined in the mask nitride and underlying pad oxide using a He and SF_6 plasma. The deep etch was performed in 45 wt% $\text{KOH}:\text{H}_2\text{O}$ solution at 80°C . The mask layer nitride and pad oxide were stripped afterwards in concentrated HF .

3.3. Wafer bonding and packaging

A silicon–silicon fusion bonding technique was used to bond the top and bottom substrates together. Both wafers were cleaned in a Piranha bath to remove any organic contamination. The wafers were then dipped in 25:1 HF solution for 10 min to ensure there was no residual nitride or oxide left on the silicon surface from earlier processes. The wafers were again dipped into a fresh Piranha solution to grow a new layer of native oxide. The two wafers were then aligned under microscope so that the entry port in the top wafer aligns to the entry flow chamber in the bottom wafer. A slight pressure was applied to achieve pre-bonding. The wafers were annealed in nitrogen ambient at 1050°C for 4 h to strengthen the bond. The bonded wafers were then diced into separate devices.

4. Device characterization

Figure 5 shows an IR (infrared) image of the bonded wafers, illustrating the entry port, exit port, and features in between the two. It is not possible to resolve all the features at this magnification; however, these features include the input finger, output finger, nanochannels, and anchor points. Figure 6

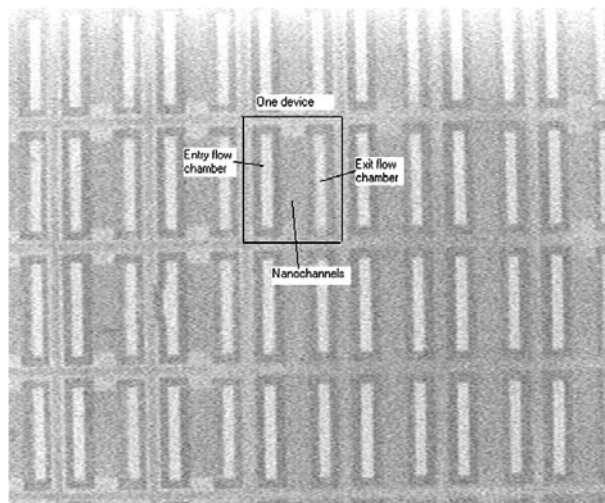


Figure 5. IR image of bonded silicon wafers. One device is outlined showing the entry port, exit port and the features in between. This includes input fingers, output fingers, anchor points, and nanochannels.

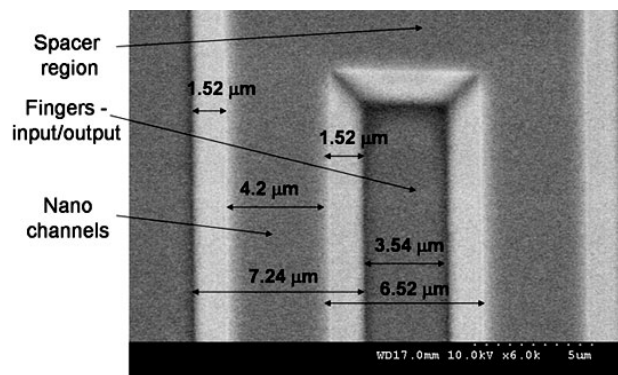


Figure 6. SEM (scanning electron microscope) image of top surface of the bottom substrate showing input/output fingers, nanochannel regions, and spacer layer. The image was taken at $\times 6k$ magnification.

shows an SEM (scanning electron microscopy) image of the top surface of the bottom substrate, showing the fingers, the nanochannel regions, and the spacer region. The image was taken at $\times 6k$ magnification. The nanochannels are between two fingers (input finger and output finger), and each finger is blocked by a spacer region at the end. The wall slope in the finger region is a result of the crystallographically selective nature of the KOH etch.

5. Diffusion characteristics

Diffusion characteristics of nanochannel delivery systems were investigated using glucose as the model molecule. The diffusion chambers were mounted on the tray of a plate shaker. The experiments were performed by applying 11 ml of a phosphate-buffered saline (PBS) solution, containing 0.2% of sodium azide, to the basolateral side of the diffusion chamber, and 0.22 ml of glucose solution (330 mg ml^{-1}) on top of it. An 8 mm diameter sphere was placed into the basolateral side of the well in order to make the solution homogeneous throughout the diffusion experiments. Plates were shaken

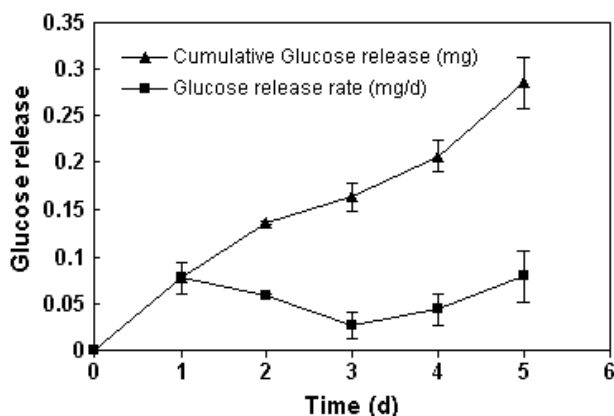


Figure 7. Glucose release profile through 60 nm channel.

at approximately 120 rpm. Samples were withdrawn at different time intervals and analysed for the presence of glucose using a Glucose-SL assay (Diagnostic Chemicals Limited, Connecticut).

Glucose diffusion through a device with 60 nm high channels was studied. Figure 7 shows the release profile of glucose over a 5 day period. The figure includes total glucose release and glucose release per day over the period investigated. A zero-order release profile was achieved within the experimental error (over three devices), allowing for maintenance of drug delivery through the nanochannels in a therapeutic window.

6. Conclusion

Nanochannel devices with 60 nm channel height were fabricated in silicon. These nanochannels are in between two directly bonded silicon wafers, and therefore pose very high mechanical strength, compared to nanopores through thin membranes. The nanochannels were defined by selectively growing oxide and then etching that oxide (sacrificial oxide). This sacrificial oxide was grown under dry thermal conditions and therefore it was possible to control the oxide thickness within ± 1 nm uniformity, and therefore the nanochannels were fabricated with less than ± 1 nm size error. The glucose flow through a 60 nm channel shows a zero-order release rate for the period investigated.

One of the barriers to use in practice is optimizing the size of the nanochannels for a desired drug delivery rate. Different

nanochannel sizes deliver different drugs with different rates. A particular drug will require to be delivered at a specified rate, and that will require changing the size of nanochannels. This barrier can be addressed with the integration of electronics on-board (development of the second device in the series of nanochannel delivery systems—nDS2). The flow through the nanochannels will then be electrically controlled and changing the voltage externally will change the flow rate.

Stability of the drug is another possible barrier. The drug should be stable in the capsule for the period of implantation.

Further investigation includes measurement of the release profile of various drugs through these nanochannels, optimization of the nanochannel size to achieve desired release rate, and integration of electronics on-board.

Acknowledgments

We would like to acknowledge Ohio MicroMD at The Ohio State University, and Berkeley Microfabrication Laboratory at the University of California, Berkeley, for use of their clean-room facilities.

References

- [1] Lewis J R and Ferrari M 2003 BioMEMS for drug delivery application *Lab-on-a-chip: Chemistry in Miniaturized Synthesis and Analysis System* ed R E Oosterbroek and A van den Berg (New York: Elsevier Science) pp 373–89
- [2] Breimer D D 1999 Future challenges for drug delivery *J. Controlled Release* **62** 3–6
- [3] Guy R, Powell M, Fix J and Park K 1996 Controlled release technologies: current status and future prospects *Pharmacol. Res.* **13** 1759
- [4] Narasimhan B and Langer R 1997 Zero-order release of micro- and macromolecules from polymeric devices: the role of the burst effect *J. Controlled Release* **47** 13–20
- [5] Holgers K M and Ljungh A 1999 Cell surface characteristics of microbiology isolates from human percutaneous implants in head and neck *Biomaterials* **20** 1319–26
- [6] Lee S C, Rueggeger M, Barners P A, Smith B R and Ferrari M 2003 Therapeutic nanodevices *The Nanotechnology Handbook* ed B Bushan (Heidelberg: Springer) pp 279–322
- [7] Desai T A, Hansford D J, Kulinsky L, Nashat A H, Rasi G, Tu J, Wang Y, Zhang M and Ferrari M 1999 Nanopore technology for biomedical application *Biomed. Microdevices* **2** 11–40
- [8] Tu J K, Huen T, Szema R and Ferrari M 1999 Filtration of sub-100 nm particles using a bulk-micromachined, direct-bonded silicon filter *Biomed. Microdevices* **1** 113–9
- [9] Sinha P M *et al* 2004 in preparation